Developmental Biology 324 (2008) 310–319

Contents lists available at ScienceDirect

Developmental Biology

journal homepage: www.elsevier.com/developmentalbiology

Role of stromal tenascin-C in mouse prostatic development and epithelial cell differentiation

Kenichiro Ishii [a,*], Kyoko Imanaka-Yoshida [b], Toshimichi Yoshida [b], Yoshiki Sugimura [a]

[a] Department of Nephro-Urologic Surgery and Andrology, Mie University Graduate School of Medicine, 2-174 Edobashi, Tsu, Mie 514-8507, Japan
[b] Department of Pathology and Matrix Biology, Mie University Graduate School of Medicine, Japan

ARTICLE INFO

Article history:
Received for publication 23 July 2008
Revised 18 September 2008
Accepted 19 September 2008
Available online 10 October 2008

Keywords:
Tenascin-C
Knockout mouse
Prostate
Epithelial–stromal interactions
Epithelial cell differentiation
Epithelial cell cluster
Binucleated cell
Androgen receptor
Tissue recombination
Urogenital sinus mesenchyme

ABSTRACT

Deregulation of epithelial–stromal interactions is considered to play a critical role in the initiation and promotion of benign prostatic hyperplasia (BPH) and prostate carcinoma (PCa). Expression of tenascin-C (TN-C), an extracellular matrix (ECM) glycoprotein, is reportedly higher in BPH and PCa as compared with normal prostate. Remodeling of the ECM alters the homeostatic balance between epithelium and stroma, resulting in physiological changes in cellular functions. To investigate the role of TN-C in prostatic development and differentiation, we evaluated the morphological phenotype of TN-C knockout (KO) mouse prostate (ventral: VP, dorsolateral: DLP, and anterior: AP) and examined tissue recombinants composed of adult mouse DLP epithelium and fetal TN-C KO urogenital sinus mesenchyme (UGM). Histological analysis showed epithelial cell clusters protruding into the ductal lumens in TN-C KO AP and DLP. Interestingly, binucleated cells appeared in epithelium of TN-C KO DLP at 8 weeks. Simultaneously, androgen receptor (AR)-positive cells were decreased in TN-C KO epithelia. Similar to the TN-C KO phenotype, protruded epithelial clusters, binucleated cells, and AR-negative nuclei were induced in DLP epithelium by recombining with TN-C KO UGM. Our results suggest that stromal TN-C might be involved in maintaining epithelial cytodifferentiation, morphogenesis, and androgen receptor expression of normal prostate glands in adult mice.

Introduction

Morphogenesis in tissue development depends on the relationships among cells, the extracellular matrix (ECM), and other support structures (Fata et al., 2004). Stromal morphogenic signals support normal epithelial differentiation and function (Simian et al., 2001). As morphogenic signals for epithelial differentiation, stromal components such as fibroblasts, myofibroblasts, and smooth muscle cells secret a number of growth factors, cytokines, and the ECM molecules. The ECM forms the extracellular environment, in cooperation with cellular ECM-receptors such as integrins and the ECM metabolism by degrading enzymes such as matrix metalloproteinases (MMPs), and their inhibitors such as tissue inhibitors of metalloproteinases (TIMPs) (Weaver et al., 2002; Green and Lund, 2005). The ECM is a heterogeneous substance composed of structural components including collagens and elastin; glycoproteins such as laminin, fibronectin, and tenascin; and proteoglycans. That the ECM environment provides significant influences on epithelial adhesion, proliferation, differentiation, and polarity, as well as apoptosis, during morphogenesis has been well studied (Ingber and Folkman, 1989; Tremblay et al., 1996; Garrison and Kyprianou, 2004).

Tenascin-C (TN-C) is a hexametric glycoprotein of the ECM produced by both epithelial and mesenchymal cells (Chiquet-Ehrismann et al., 1986; Orend and Chiquet-Ehrismann, 2006). During embryogenesis and morphogenesis, TN-C appears at active sites of tissue remodeling and its expression seems to be regulated by reciprocal interactions between epithelial and mesenchymal components via paracrine factors such as transforming growth factor β (TGFβ) (Thompson et al., 2006). TN-C expression is strictly limited in adults but prominently reappears under pathologic conditions, i.e. the expression of TN-C is induced by proliferating epithelia (normal and particularly malignant) and is downregulated with their differentiation (Vollmer et al., 1994b).

The prostate is an organ which is induced by embryonic mesenchyme, fibroblasts and myofibroblasts, during its development and differentiation (Cunha et al., 1980). In mice, prostatic buds develop from the urogenital sinus on 17 days of gestation (Cunha, 1976). TN-C appears in mesenchyme surrounding the urogenital sinus epithelium, which undergoes major morphogenic changes including the formation of prostatic buds (Takeda et al., 1988). The dynamics of TN-C expression are closely associated with the development and maturation of the prostate gland (Shiraishi et al., 1994). However, the precise

* Corresponding author. Fax: +81 59 231 5203.
E-mail address: kenishii@clin.medic.mie-u.ac.jp (K. Ishii).

0012-1606/$ – see front matter © 2008 Elsevier Inc. All rights reserved.
doi:10.1016/j.ydbio.2008.09.029

mechanisms of TN-C-directed epithelial cytodifferentiation and morphogenesis in prostate are little understood as yet.

To investigate the role of TN-C as a stromal morphogenic signal in prostatic development and differentiation, we first evaluated the morphological phenotype of TN-C knockout (TN-C KO) mouse prostate. Next, we examined tissue recombinants composed of adult mouse DLP epithelium and fetal TN-C KO mouse urogenital sinus mesenchyme (UGM) to confirm the morphological phenotype observed in TN-C KO mouse prostate was due to stromal TN-C. In regard to the role of TN-C as a stromal morphogenic signal that drives epithelial cell differentiation, we further investigated the effects of stromal TN-C on the adult urothelial transdifferentiation to prostatic epithelia in tissue recombination.

Materials and methods

Antibodies

Rabbit polyclonal anti-androgen receptor (AR) (N-20) and mouse monoclonal anti-Ki-67 (clone MIB-1) antibodies were purchased from Santa Cruz Biotechnology, Inc. (Santa Cruz, CA, USA) and DakoCytomation, Inc. (Copenhagen, Denmark), respectively. Mouse monoclonal anti-E-cadherin (clone 36) antibody was purchased from BD Transduction Laboratories, Inc. (Lexington, KY, USA). Mouse monoclonal anti-α-actin, smooth muscle (αSMA; A5228) and mouse monoclonal anti-γ-actin (clone B4) antibodies were purchased from Sigma-Aldrich, Inc. (St. Louis, MO, USA) and ICN Biomedicals, Inc. (Costa Mesa, CA, USA), respectively. Rabbit polyclonal anti-cleaved caspase-3 (Asp175) and mouse monoclonal anti-uroplakin III (clone AU1) antibodies were purchased from Cell Signaling Technology, Inc. (Beverly, MA, USA) and Research Diagnostics, Inc. (Concord, MA, USA), respectively. Rabbit polyclonal anti-human TN-C antibody was established and characterized as previously reported (Imanaka-Yoshida et al., 2001).

Animals

TN-C null mice, originally generated by Saga et al. (1992) were backcrossed with BALB/c strain mice. WT littermates were used as controls. All animals were maintained in a specific pathogen-free environment under controlled conditions of light and humidity. Food and tap water were provided *ad libitum*.

Termination and prostatic lobe dissection

All animals were sacrificed at specified time points by an overdose of isoflurane followed by cervical dislocation. After measurement of body weight and urogenital weight, prostates were separated into three lobes: anterior prostate (AP), dorsolateral prostate (DLP), and ventral prostate (VP) (Sugimura et al., 1986). Wet weights were determined for each prostatic lobe and the seminal vesicle (SV). For histological and immunohistochemical analyses, tissues were fixed in 10% neutral-buffered formalin (Wako Pure Chemical Industries, Osaka, Japan) at room temperature overnight and then processed and embedded in paraffin in accordance with standard procedures.

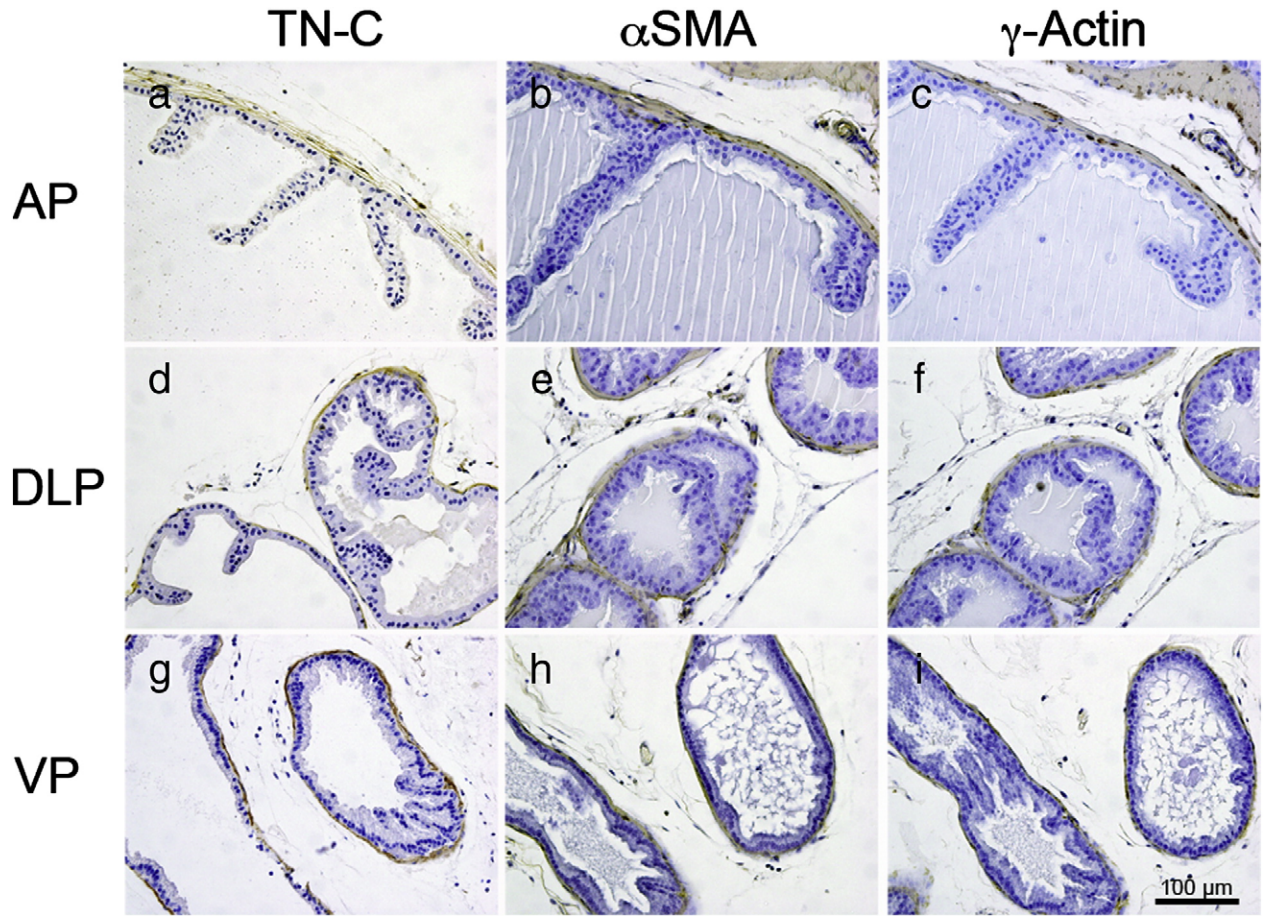

Fig. 1. Localization of TN-C in adult mouse prostate. Localization of TN-C (a, d, and g) was assessed by immunostaining in 17-week-old WT mouse prostate. Immunoreactivities for αSMA (b, e, and h) and γ-actin (c, f, and i) were compared to TN-C expression. The corresponding sections from AP, DLP, and VP are shown in panels a–c, d–f, and g–i, respectively. Scale bar = 100 μm, magnification ×200.

Tissue recombination

Mouse UGM was prepared from 16-day embryonic mouse fetuses (plug date denoted as day 0) of pregnant WT or TN-C KO mice as previously described (Ishii et al., 2005). Briefly, urogenital sinuses were dissected from the fetuses and separated into epithelial and mesenchymal components by tryptic digestion and mechanical separation. Prostatic organoids of WT DLP or adult WT bladder urothelial cells were recombined with WT or TN-C KO UGM in neutralized type I rat tail collagen gels, and then tissue recombinants were grafted beneath the renal capsule of 8-week-old adult homozygous athymic CD-1 male nude mice (CLEA Japan, Inc., Tokyo, Japan).

Histopathology and immunohistochemistry

Serial sections (3 μm thick) were cut on a Leica RM2125 rotary microtome (Leica Microsystems, Wetzlar, Germany) and mounted on glass slides. Sections were deparaffinized in Histoclear (National Diagnostic, Atlanta, GA, USA) and hydrated in graded alcoholic solutions and running tap water. For histopathology, standard H&E and Masson's trichrome staining were carried out. Next, immunohistochemical staining was performed with a Vectastain ABC *Elite* kit (Vector laboratories Inc., Burlingame, CA, USA) following our protocol. After deparaffinization and hydration, endogenous peroxidase activity was blocked with 0.3% hydrogen peroxide in methanol for 20 min. After extensive washing in tap water, antigen retrieval was performed using 10 mM sodium citrate buffer of pH 6.0 for AR, Ki-67, and cleaved caspase-3. Antigen Unmasking Solution (Vector laboratories Inc., Burlingame, CA, USA) and 1.3 mg/mL pepsin solution were used for E-cadherin and uroplakin, and TN-C, respectively. For αSMA and γ-actin, antigen retrieval was not performed. Following a period of cooling and then rinsing in phosphate-buffered saline (PBS), the sections were incubated in blocking solution for at least 30 min at room temperature. The sections were then incubated with primary antibodies at 4 °C overnight. After incubation with primary antibodies, sections were incubated with appropriate biotinylated secondary anti-

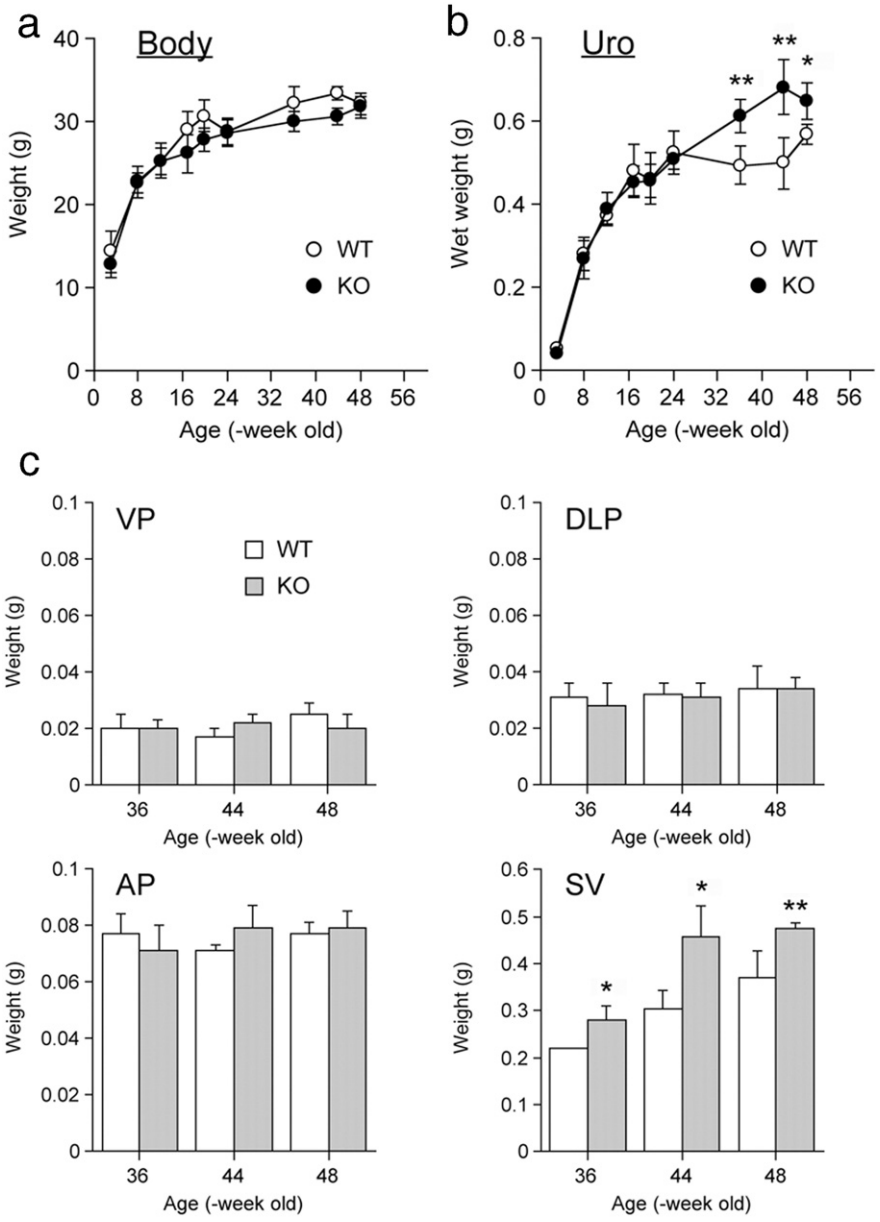

Fig. 2. No significant difference in prostatic weight of TN-C KO mouse. Body weight (a) and wet weight of mouse urogenital tract (b) from WT (○) and TN-C KO (●) were weighted at various ages. (c) Wet weights of microdissected lobes from WT (□) and TN-C KO (■) are indicated for various ages. VP: ventral prostate, DLP: dorsolateral prostate, AP: anterior prostate, SV: seminal vesicle. Values represent the means ± S.D. * $p<0.05$, ** $p<0.01$ versus WT.

mouse, anti-rabbit, or anti-rat immunoglobulin included in the ABC *Elite* kit for 30 min at room temperature. The antigen–antibody reaction was visualized using 3,3′-diaminobenzidine tetrahydrochloride (DAB) as a substrate. Sections were counterstained with hematoxylin and examined by light microscopy. Anti-AR, E-cadherin, Ki-67, αSMA, γ-actin, cleaved caspase-3, uroplakin, and TN-C were used at dilutions of 1:300, 1:3000, 1:100, 1:10,000, 1:1000, 1:400, 1:50, and 1:1000, respectively. The number of binucleated cells was determined by E-cadherin immunostaining in ten separate microscopic fields (×400) from each tissue specimen.

Statistical analysis

The results were expressed as the means±S.D. Differences between the two groups were determined using Student's *t*-test. Values of $p<0.05$ were considered statistically significant.

Results

Expression of TN-C in prostate of WT mice

We separated all mouse prostates from 17-week-old into three lobes each: anterior prostate (AP), dorsolateral prostate (DLP), and ventral prostate (VP), as previously reported (Sugimura et al., 1986). In WT mouse, ducts of all prostatic lobes were lined by luminal secretory epithelial cells with basally located nuclei (Fig. 1). Immunostaining for αSMA and smooth muscle γ-actin, a late marker for smooth muscle differentiation (Qian et al., 1996), showed that prostatic ducts were generally surrounded with thin stromal smooth muscle layers (Figs. 1b, c, e, f, h, i). TN-C was localized beneath the basement membrane surrounding prostatic ducts as previously reported in rat prostate (Vollmer et al., 1994a) (Figs. 1a, d, g).

Table 1
Comparisons of cell proliferation and apoptotic incidence between WT and TN-C KO mice

	WT		TN-C KO	
	Epi	Stroma	Epi	Stroma
Cell proliferation (%)				
AP	2.4±1.7	1.1±2.5	0.9±0.4	4.1±5.0
DLP	0.3±0.7	1.1±2.5	0.3±0.4	0±0
VP	0.9±1.3	0±0	1.6±1.6	0±0
Apoptosis (%)				
AP	0.5±1.1	0±0	0±0	0±0
DLP	0±0	0±0	0±0	0±0
VP	0±0	0±0	0.4±0.9	0±0

Cell proliferation and apoptotic incidence in 17-week-old mice were analyzed by Ki-67 immunostaining and cleaved caspase-3 immunostaining, respectively. Values represent the means±S.D. from at least 5 ducts.

Morphological phenotype of TN-C KO mouse prostate

There was no significant difference in body weights between WT and TN-C KO mice (Fig. 2a). Wet weights of urogenital tract including all prostatic lobes and the SV in TN-C KO mouse were significantly heavier than those in WT mouse between 36 weeks and 48 weeks of age ($p<0.05$) (Fig. 2b). The SV weights in TN-C KO mouse were significantly heavier than those in WT mouse ($p<0.05$) (Fig. 2c),

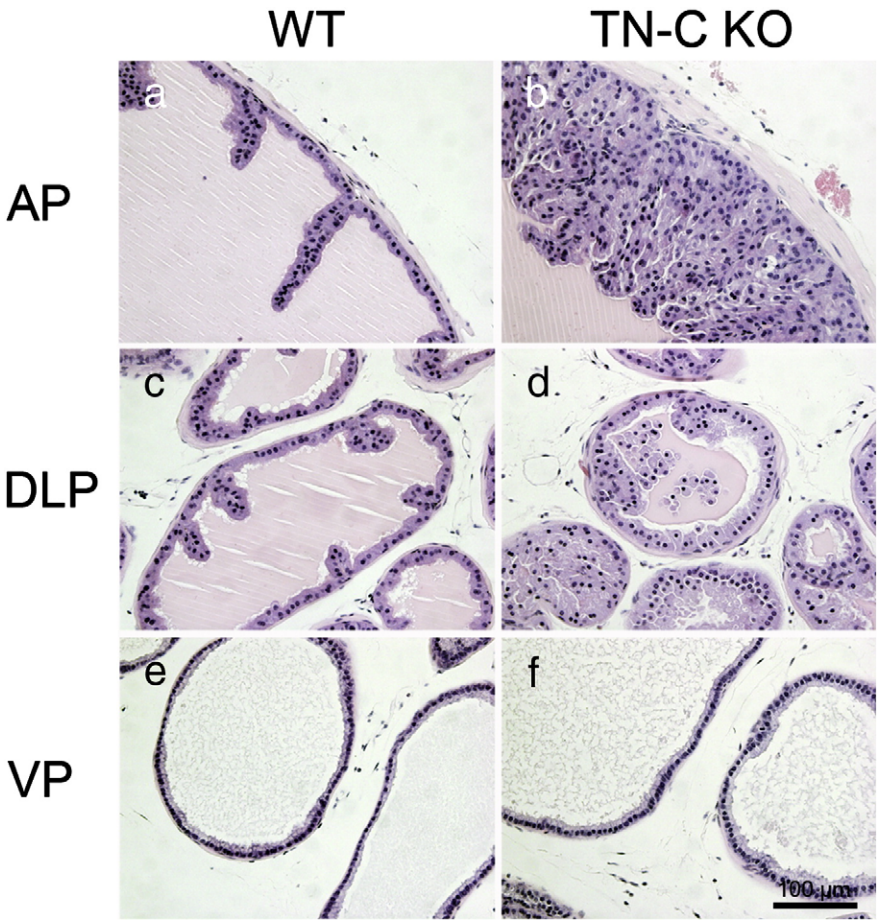

Fig. 3. Morphological phenotype of TN-C KO mouse prostate. All sections from 17-week-old mice were H&E stained. The corresponding sections from AP, DLP, and VP are shown in panels a, c, and e for WT, and in panels b, d, f for TN-C KO. Scale bar=100 μm, magnification ×200.

although there were no significant differences among individual prostatic lobe weights between WT and TN-C KO mice.

In TN-C KO mouse, multilayered epithelial clusters protruded into the ductal lumens in the AP (Fig. 3b) and also in the DLP, but to a lesser extent (Fig. 3d). The multilayered epithelium appeared at 8 weeks, and was maintained thereafter to at least 48 weeks. Although the stroma in TN-C KO prostate tended to be thicker than that in WT prostate, there was no aggressive phenotype of stromal component such as hypercellular stroma or spindled stroma (Ishii et al., 2005). Accumulation of collagen was not observed by Masson's trichrome staining (data not shown). No significant increase of cell proliferation or decrease of apoptotic incidence in epithelial or stromal component was found by analyses of Ki-67 labeling index or caspase-3 labeling index when examined at 17 weeks, respectively (Table 1). The TN-C KO VP appeared morphologically normal as compared with the WT VP (Figs. 3e, f). In the TN-C KO SV, there was no apparent morphological difference such as epithelial hyperplasia or hypercellular stroma (data not shown).

Histological analysis in TN-C KO mouse prostate

Binucleated cells, having two nuclei in individual epithelial cells surrounding E-cadherin-positive membrane, were shown in glands of the TN-C KO AP and DLP (Figs. 4b, d). In WT mouse, however, binucleated cells were rarely observed (Figs. 4a, c). The number of binucleated cells in the TN-C KO DLP was significantly increased from 8 weeks to 48 weeks of age, accompanied with multilayered epithelial growth ($p<0.05$) (Fig. 4e).

The expression of AR was detected in nuclei of both epithelial and stromal cells of the WT AP and DLP (Figs. 5a, c). Interestingly, in TN-C KO mice, AR-positive epithelial cells were decreased in the AP lobe, and most epithelial cells in the DLP were AR-negative; stromal cells surrounding the ducts were AR-positive ($p<0.01$) (Figs. 5d, e). The percentage of AR-negative epithelial cells in the AP was quite low compared to that in the DLP in TN-C KO mice (Figs. 5b, e). No significant difference in AR expression was observed between WT and TN-C KO VP (Fig. 5e).

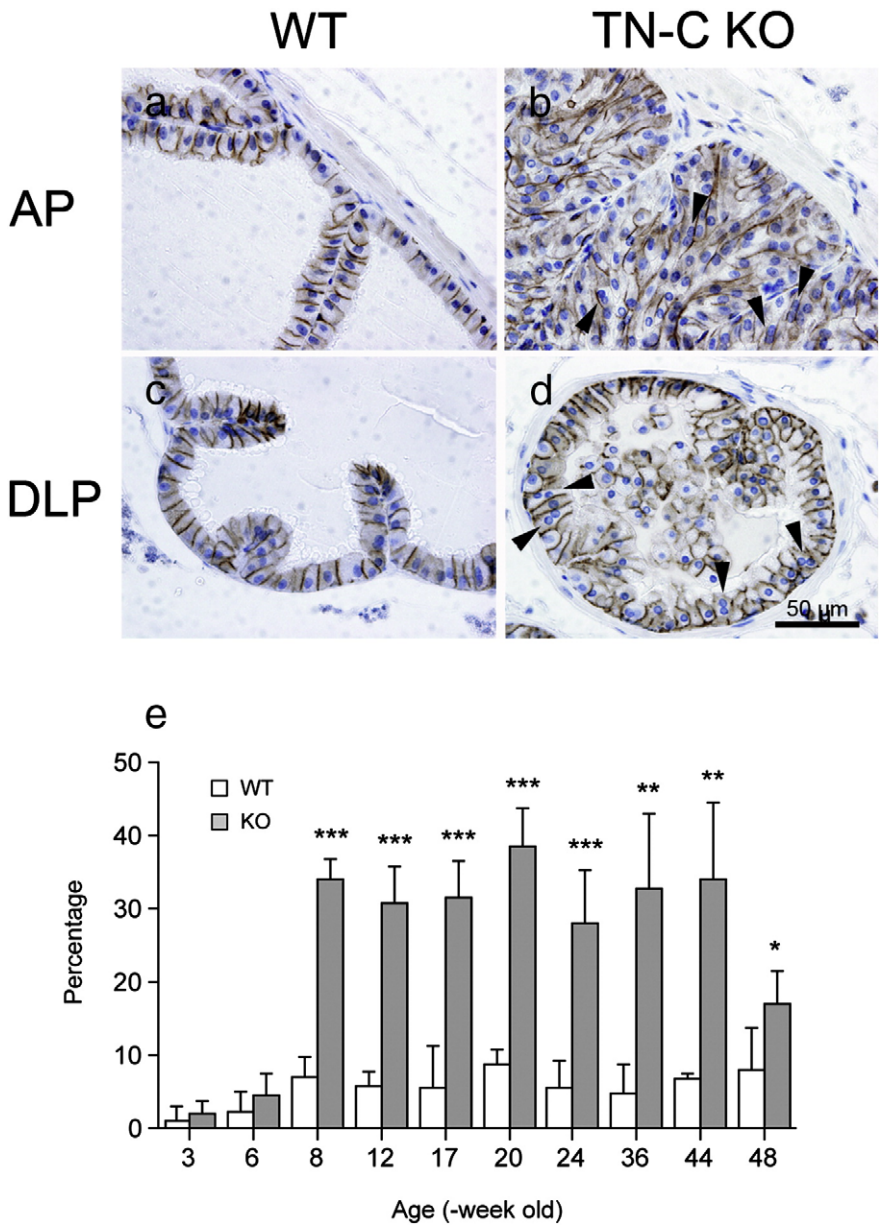

Fig. 4. Appearance of binucleated cells in TN-C KO mouse prostate. (a–d) The histopathology of WT and TN-C KO mouse prostate was examined with E-cadherin immunostaining. The corresponding sections from AP and DLP are shown in panels a and c for WT, and in b and d for TN-C KO. Arrowheads indicate the binucleated cells. Scale bar = 50 μm, magnification ×400. (e) The number of binucleated cells in each DLP duct of WT (□) and TN-C KO (■) was counted at various ages. Values represent the means ± S.D. from at least 5 ducts. * $p<0.05$, ** $p<0.01$, *** $p<0.001$ versus WT.

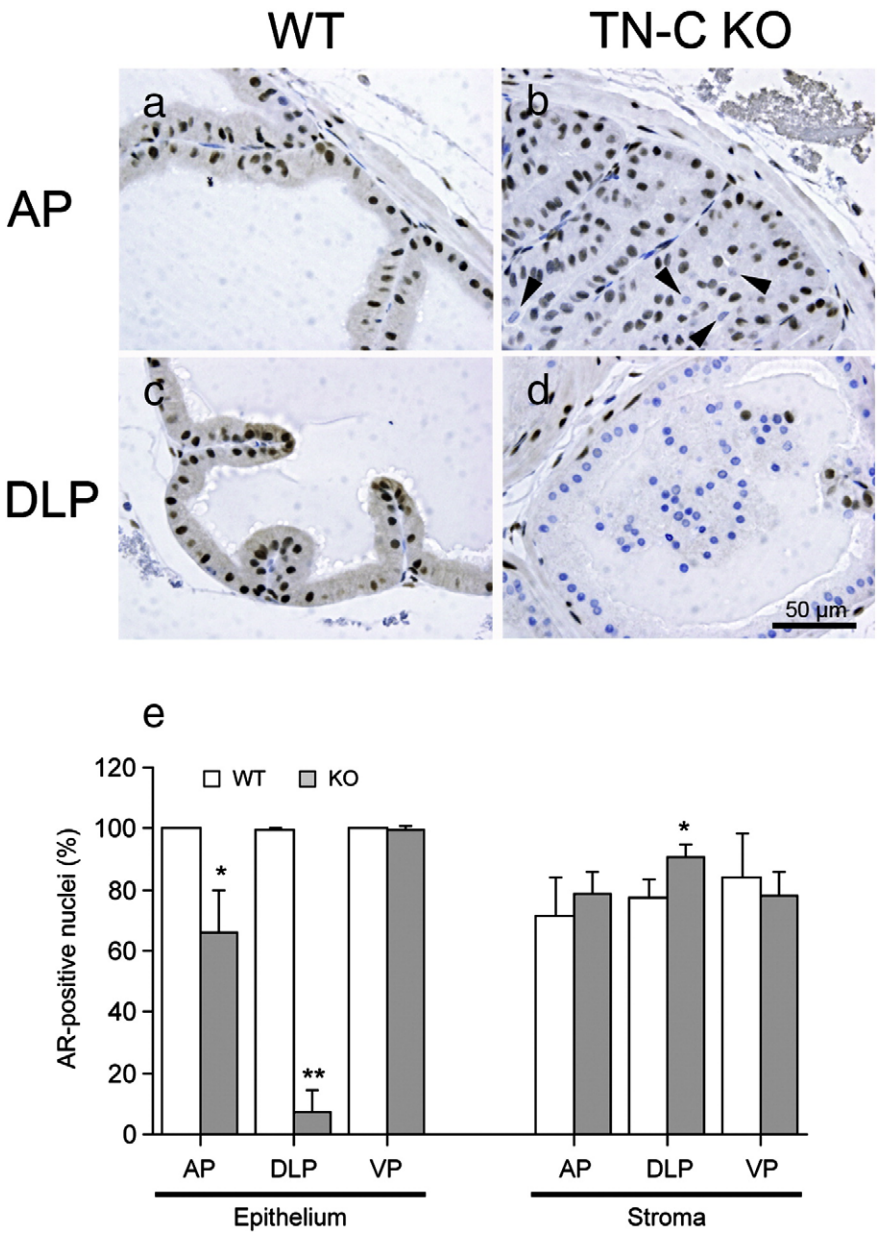

Fig. 5. Loss of AR expression in the epithelium of TN-C KO mouse prostate. (a–d) AR expression was assessed by immunostaining in WT and TN-C KO mouse prostate. The corresponding sections from AP and DLP are shown in panels a and c for WT, and in panels b and d for TN-C KO. Arrowheads indicate the AR-negative nuclei. Scale bar = 50 μm, magnification ×400. (e) The number of AR-positive nuclei in each prostatic duct of WT (□) and TN-C KO (■) was counted at 17 weeks of age, and then the percentage of AR-positive cells was calculated. Values represent the means ± S.D. for at least 5 ducts. * $p<0.01$, ** $p<0.0001$ versus WT.

Tissue recombination with fetal TN-C KO UGM

To examine whether TN-C deficiency in prostatic stroma affected epithelial growth and differentiation, we performed tissue recombination between adult WT DLP epithelium and UGM of WT or TN-C KO mice, and then grafted recombinants beneath the renal capsule (Figs. 6a, b). Recombinants were examined at 4 weeks postgrafting. Control recombinants with WT UGM showed normal-appearing prostatic glandular epithelium exhibiting normal secretory differentiation (Fig. 6c) and with a thin layer of stroma similar to that of intact WT mouse prostate, as described previously (Ishii et al., 2005).

In contrast, tissue recombinants prepared with TN-C KO UGM and adult WT prostatic epithelium showed morphological phenotypes including multilayered epithelial clusters, binucleated cells, and AR-negative nuclei, similar to those in TN-C KO mouse prostate (Figs. 6d, f, h). Histological analysis such as αSMA immunostaining and Masson's trichrome staining showed no significant difference in the stromal component adjacent to prostatic epithelia between WT and TN-C KO recombinants (data not shown). Thus, these findings indicate that TN-C-null mesenchymal components can induce the morphological changes in WT prostate glands in tissue recombinants similar to that seen in TN-C KO mice.

To investigate whether TN-C-null mesenchymal components can induce urothelial transdifferentiation to prostatic epithelia, we next performed tissue recombination between adult WT bladder urothelial cells and UGM of WT or TN-C KO mice (Fig. 7). Control recombinants with WT UGM showed induction of normal-appearing prostatic glandular structure from adult bladder urothelial cells, as expected (Figs. 7a, c, e, g). In contrast, tissue recombinants with TN-C KO UGM showed morphological differences with no prostatic secretion in the lumen (Figs. 7b, d). Detailed histological analyses showed that some AR-positive epithelial cells appeared but uroplakin-positive bladder urothelial cells still remained in the resultants with TN-C KO UGM+

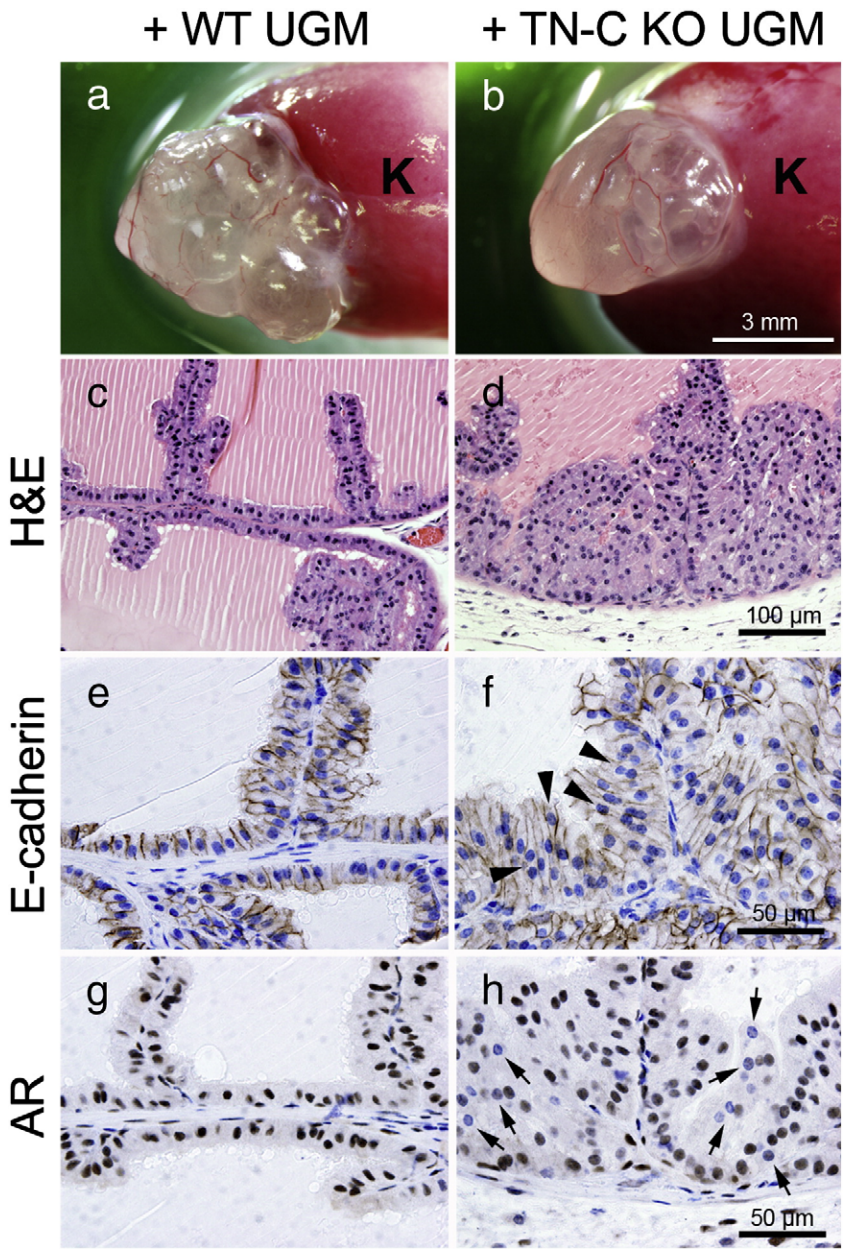

Fig. 6. Tissue recombinants composed of adult WT DLP epithelium and fetal TN-C KO UGM. (a–d) Gross appearances of WT and TN-C KO recombinants are shown in panels a and b, respectively. Vascularized cystic mass is observed on the host kidney (K). The histopathology was examined with H&E staining shown in c for WT and d for TN-C KO recombinants. Scale bar = 100 μm, magnification ×200. (e–h) Detailed histopathological characteristics were examined with expression of E-cadherin (e and f) and AR (g and h). The corresponding sections from tissue recombinants are shown in panels e and g for WT, and in panels f and h for TN-C KO. Arrowheads and arrows indicate the binucleated cells and the AR-negative nuclei, respectively. Scale bar = 50 μm, magnification ×400.

bladder epithelium tissue recombinants (Figs. 7f, h). These results indicate that stromal TN-C participates in urothelial transdifferentiation to prostatic epithelia.

Discussion

TN-C is often induced in response to mesenchymal–epithelial interactions that initiate organogenesis and morphogenesis (Chiquet-Ehrismann et al., 1986). Mesenchymal–epithelial interactions play crucial roles in morphogenesis and cytodifferentiation in the development of the prostate (Cunha, 1976). However, it has been proposed that TN-C might not be involved in the early morphogenesis of the prostatic buds, because little TN-C was detected in the mesenchyme around developing prostatic buds (Takeda et al., 1988). In adult prostate, stroma composed of smooth muscle cells also interact with glandular epithelia. These stromal–epithelial interactions maintain functional differentiation and growth-quiescence of glandular epithelia (Hayward et al., 1997). Deregulation of the stromal–epithelial interactions is considered to be responsible for the initiation and/or promotion of prostatic diseases such as benign prostatic hyperplasia (BPH) and prostate carcinoma (PCa) (Olumi et al., 1999; Bhowmick et al., 2004). Since increased TN-C expression has been observed in these lesions (Ibrahim et al., 1993; Xue et al., 1998), many recent studies have focused on the role of TN-C in prostate cancer progression (Tomas et al., 2006; Tuxhorn et al., 2002).

To investigate TN-C functions in organogenesis and morphogenesis, TN-C KO mice were independently generated by two different groups (Saga et al., 1992; Forsberg et al., 1996). Both groups have reported the same findings, that TN-C deficient mice undergo normal in development and have a normal life span and fertility in mice. TN-C

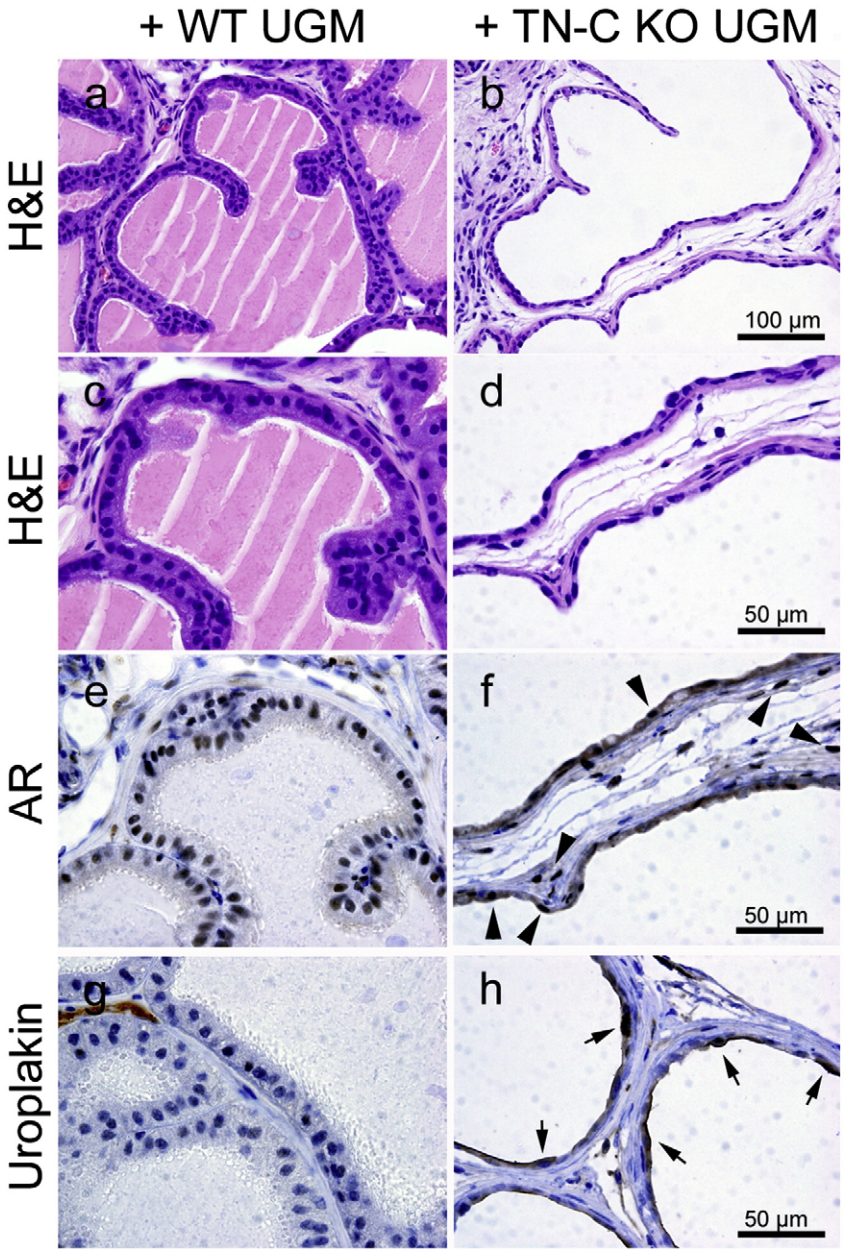

Fig. 7. Tissue recombinants composed of adult WT bladder urothelial cells and fetal TN-C KO UGM. (a–d) The histopathology was examined with H&E staining shown in panels a and c for WT or panels b and d for TN-C KO recombinants. Scale bar = 100 μm, magnification ×200, Scale bar = 50 μm, magnification ×400. (e–h) Detailed histopathological characteristics were examined with expression of AR (e and f) and uroplakin (g and h). The corresponding sections from tissue recombinants are shown in panels e and g for WT, and in panels f and h for TN-C KO. Arrowheads and arrows indicate the AR-positive cells and the uroplakin-positive cells, respectively. Scale bar = 50 μm, magnification ×400.

null mice did not show any morphological phenotype in the principal organs such as heart, lung, thymus, and cerebellum (Saga et al., 1992; Imanaka-Yoshida et al., 2003). However, more detailed investigations have shown differences in specific cell behavior and response to external stimuli in adult (Ohta et al., 1998; Fukamauchi et al., 1997; Tamaoki et al., 2005). Decreased bronchial branching and enlarged airspaces have been found in lung development of TN-C KO mice (Roth-Kleiner et al., 2004). Recently we have also reported that TN-C deficiency attenuates allergic inflammation in bronchial asthma and liver fibrosis in chronic hepatitis (Nakahara et al., 2006; El-Karef et al., 2007).

The present study demonstrated that the prostate in TN-C KO mice developed and grew almost normally. However, with careful microscopical analysis, we observed multilayered ductal epithelia and binucleated cells in AP and DLP lobes of TN-C KO mice. Tissue recombinants using fetal TN-C KO UGM and adult prostatic epithelia elicited similar morphological changes in prostatic epithelia, indicating that deficiency of stromal TN-C causes the glandular phenotypes. In addition, it was found that a certain population of these abnormal glandular epithelia failed to express AR proteins both *in vivo* and in TN-C KO UGM+ WT prostatic epithelium tissue recombinants. Therefore, it is suggested that stromal TN-C plays an important role in maintaining adult prostatic ductal morphology. The SV weights in TN-C KO mouse were significantly heavier than those in WT mouse, while the glandular change was not observed. Epithelial clusters of AP and DLP protruding into ductal lumen may cause obstruction, followed by retention of seminal fluid in the SV.

In regard to the role of TN-C as a stromal morphogenic signal that drives epithelial cell differentiation, we further investigated the effects of stromal TN-C on the adult urothelial transdifferentiation to prostatic epithelia in tissue recombination. AR-positive UGM has been demonstrated to induce the prostatic development and morphogen-

esis by action of androgens (Thompson et al., 1986). For example, UGM can induce prostatic epithelial development and morphogenesis in AR-negative endoderm-derived epithelia such as bladder and urethra (Cunha et al., 1983). The tissue recombinants composed of adult WT bladder urothelial cells and TN-C KO UGM showed that TN-C null UGM was not able to completely induce the bladder urothelial cells to undergo prostatic differentiation (Fig. 7). In addition, there was no prostatic secretion in the lumen. These results strongly suggest that stromal TN-C may play roles not only in prostatic epithelial cytodifferentiation but also in urothelial transdifferentiation to prostatic epithelia. Shima et al. (1995) previously reported that UGM-derived factors including growth factors and cytokines might regulate the epithelial cell differentiation in this process. Our results have proposed the idea that the adult urothelial transdifferentiation to prostatic epithelia requires ECM-signaling such as stromal TN-C.

Mature prostate tissue does not actively proliferate, and there is little cellular turnover in the adult prostate. It has been well known that mice do not spontaneously develop pathologic conditions such as BPH even in aged mouse prostate. However, several reports have shown prostatic epithelial hyperplasia in genetically modified mice. Mice carrying mutation of *Nkx3.1*, which is essential for normal morphogenesis and function of the prostate, showed prostatic epithelial hyperplasia and dysplasia (Bhatia-Gaur et al., 1999). In ERβ−/− mouse VP, there were increased epithelial proliferation, decreased apoptosis, and accumulation of incompletely differentiated cells, resulting in epithelial cellular hyperplasia (Imamov et al., 2004). The prostatic epithelium of PKS mice, which is a transgenic mouse with target overexpression of FGF-7/KGF in prostatic epithelium, was found to be hyperplastic (Foster et al., 2002). In TN-C KO mice, despite the significant increased mass of epithelial cell clusters and the number of binucleated cells (in AP and DLP), Ki-67 labeling indices of epithelial cells were very low in TN-C KO mice at 17 weeks and were similar to that of WT mice. In addition, there was no significant difference in apoptotic incidence at all stages examined.

In adult prostate of WT mice, TN-C is deposited along the stromal–epithelial interface. TN-C stimulates reorganization of actin stress fibers and disassembly of focal adhesion complexes, causing a weak adhesive state of the cells to the matrix (Murphy-Ullrich et al., 1991; Imanaka-Yoshida et al., 2001), which would facilitate changes of cell morphology. TN-C deficiency might make de-adhesion of the cells from the basement membrane difficult. The cells might become binucleated when mitosis without proper cytokinesis occurs (Stukenberg, 2004). In TN-C null condition, rigid adhesion of epithelial cells to the matrix could reduce the spontaneous detachment of the cells, resulting in multilayered epithelia following delayed turnover.

This study showed that deficiency of stromal TN-C signaling on mouse prostatic epithelium reduced or abolished expression of AR protein. An important feature of the normal adult prostate gland is the lack of proliferation even in the presence of growth-stimulating androgens. Ductal morphogenesis, epithelial cytodifferentiation, and proliferation/apoptosis are regulated by androgens acting through stromal AR, while epithelial AR is responsible for maintaining the differentiated phenotype and overall homeostasis of the glands (Hayward et al., 1997). Selective removal of AR signaling in luminal and basal epithelial cells stimulates mitogenesis and impaired functional differentiation in the growth quiescent adult prostate even though this effect was only seen late in life (Wu et al., 2007). In regard to cell adhesion, it is considered that rigid adhesion to basement membrane exerts a negative regulatory effect on AR expression and that the reduction in cell adhesion is a requirement for AR protein expression in the normal prostate epithelium (Knudsen and Miranti, 2006). Taken together with these findings, it is proposed that solid cell adhesion to the substratum caused by deficiency of de-adhesive molecule TN-C triggers loss of AR expression and cell differentiation in prostatic epithelium. Further investigation is necessary to determine the molecular mechanisms by which stromal TN-C deficiency induces multilayered, binucleated, and AR-negative ductal epithelial cells of the prostate.

Acknowledgments

We especially appreciate the advice and expertise of Drs. Teruyo Sakakura, Simon W. Hayward, Robert J. Matusik, and Neil A. Bhowmick. We also thank Mrs. Hiroko Nishii, Mari Hara, and Akiyo Sekimoto for technical support. This work was supported by Grants-in-Aid from the Ministry of Education for Science and Culture of Japan (17791072, 19591841, 19659412).

References

Bhatia-Gaur, R., Donjacour, A.A., Sciavolino, P.J., Kim, M., Desai, N., Young, P., Norton, C.R., Gridley, T., Cardiff, R.D., Cunha, G.R., Abate-Shen, C., Shen, M.M., 1999. Roles for Nkx3.1 in prostate development and cancer. Genes Dev. 13, 966–977.

Bhowmick, N.A., Chytil, A., Plieth, D., Gorska, A.E., Dumont, N., Shappell, S., Washington, M.K., Neilson, E.G., Moses, H.L., 2004. TGF-beta signaling in fibroblasts modulates the oncogenic potential of adjacent epithelia. Science 303, 848–851.

Chiquet-Ehrismann, R., Mackie, E.J., Pearson, C.A., Sakakura, T., 1986. Tenascin: an extracellular matrix protein involved in tissue interactions during fetal development and oncogenesis. Cell 47, 131–139.

Cunha, G.R., 1976. Epithelial–stromal interactions in development of the urogenital tract. Int. Rev. Cytol. 47, 137–194.

Cunha, G.R., Chung, L.W., Shannon, J.M., Reese, B.A., 1980. Stromal–epithelial interactions in sex differentiation. Biol. Reprod. 22, 19–42.

Cunha, G.R., Fujii, H., Neubauer, B.L., Shannon, J.M., Sawyer, L., Reese, B.A., 1983. Epithelial–mesenchymal interactions in prostatic development. I. Morphological observations of prostatic induction by urogenital sinus mesenchyme in epithelium of the adult rodent urinary bladder. J. Cell Biol. 96, 1662–1670.

El-Karef, A., Yoshida, T., Gabazza, E.C., Nishioka, T., Inada, H., Sakakura, T., Imanaka-Yoshida, K., 2007. Deficiency of tenascin-C attenuates liver fibrosis in immune-mediated chronic hepatitis in mice. J. Pathol. 211, 86–94.

Fata, J.E., Werb, Z., Bissell, M.J., 2004. Regulation of mammary gland branching morphogenesis by the extracellular matrix and its remodeling enzymes. Breast Cancer Res. 6, 1–11.

Forsberg, E., Hirsch, E., Frohlich, L., Meyer, M., Ekblom, P., Aszodi, A., Werner, S., Fassler, R., 1996. Skin wounds and severed nerves heal normally in mice lacking tenascin-C. Proc. Natl. Acad. Sci. U. S. A. 93, 6594–6599.

Foster, B.A., Evangelou, A., Gingrich, J.R., Kaplan, P.J., DeMayo, F., Greenberg, N.M., 2002. Enforced expression of FGF-7 promotes epithelial hyperplasia whereas a dominant negative FGFR2iiib promotes the emergence of neuroendocrine phenotype in prostate glands of transgenic mice. Differentiation 70, 624–632.

Fukamauchi, F., Wang, Y.J., Mataga, N., Kusakabe, M., 1997. Paradoxical behavioral response to apomorphine in tenascin-gene knockout mouse. Eur. J. Pharmacol. 338, 7–10.

Garrison, J.B., Kyprianou, N., 2004. Novel targeting of apoptosis pathways for prostate cancer therapy. Curr. Cancer Drug Targets 4, 85–95.

Green, K.A., Lund, L.R., 2005. ECM degrading proteases and tissue remodelling in the mammary gland. Bioessays 27, 894–903.

Hayward, S.W., Rosen, M.A., Cunha, G.R., 1997. Stromal–epithelial interactions in the normal and neoplastic prostate. Br. J. Urol. 79 (Suppl. 2), 18–26.

Ibrahim, S.N., Lightner, V.A., Ventimiglia, J.B., Ibrahim, G.K., Walther, P.J., Bigner, D.D., Humphrey, P.A., 1993. Tenascin expression in prostatic hyperplasia, intraepithelial neoplasia, and carcinoma. Hum. Pathol. 24, 982–989.

Imamov, O., Morani, A., Shim, G.J., Omoto, Y., Thulin-Andersson, C., Warner, M., Gustafsson, J.A., 2004. Estrogen receptor beta regulates epithelial cellular differentiation in the mouse ventral prostate. Proc. Natl. Acad. Sci. U. S. A. 101, 9375–9380.

Imanaka-Yoshida, K., Hiroe, M., Nishikawa, T., Ishiyama, S., Shimojo, T., Ohta, Y., Sakakura, T., Yoshida, T., 2001. Tenascin-C modulates adhesion of cardiomyocytes to extracellular matrix during tissue remodeling after myocardial infarction. Lab. Invest. 81, 1015–1024.

Imanaka-Yoshida, K., Matsumoto, K., Hara, M., Sakakura, T., Yoshida, T., 2003. The dynamic expression of tenascin-C and tenascin-X during early heart development in the mouse. Differentiation 71, 291–298.

Ingber, D.E., Folkman, J., 1989. How does extracellular matrix control capillary morphogenesis? Cell 58, 803–805.

Ishii, K., Shappell, S.B., Matusik, R.J., Hayward, S.W., 2005. Use of tissue recombination to predict phenotypes of transgenic mouse models of prostate carcinoma. Lab. Invest. 85, 1086–1103.

Knudsen, B.S., Miranti, C.K., 2006. The impact of cell adhesion changes on proliferation and survival during prostate cancer development and progression. J. Cell. Biochem. 99, 345–361.

Murphy-Ullrich, J.E., Lightner, V.A., Aukhil, I., Yan, Y.Z., Erickson, H.P., Hook, M., 1991. Focal adhesion integrity is downregulated by the alternatively spliced domain of human tenascin. J. Cell Biol. 115, 1127–1136.

Nakahara, H., Gabazza, E.C., Fujimoto, H., Nishii, Y., D'Alessandro-Gabazza, C.N., Bruno, N.E., Takagi, T., Hayashi, T., Maruyama, J., Maruyama, K., Imanaka-Yoshida, K., Suzuki, K., Yoshida, T., Adachi, Y., Taguchi, O., 2006. Deficiency of tenascin C

attenuates allergen-induced bronchial asthma in the mouse. Eur. J. Immunol. 36, 3334–3345.
Ohta, M., Sakai, T., Saga, Y., Aizawa, S., Saito, M., 1998. Suppression of hematopoietic activity in tenascin-C-deficient mice. Blood 91, 4074–4083.
Olumi, A.F., Grossfeld, G.D., Hayward, S.W., Carroll, P.R., Tlsty, T.D., Cunha, G.R., 1999. Carcinoma-associated fibroblasts direct tumor progression of initiated human prostatic epithelium. Cancer Res. 59, 5002–5011.
Orend, G., Chiquet-Ehrismann, R., 2006. Tenascin-C induced signaling in cancer. Cancer Lett. 244, 143–163.
Qian, J., Kumar, A., Szucsik, J.C., Lessard, J.L., 1996. Tissue and developmental specific expression of murine smooth muscle gamma-actin fusion genes in transgenic mice. Dev. Dyn. 207, 135–144.
Roth-Kleiner, M., Hirsch, E., Schittny, J.C., 2004. Fetal lungs of tenascin-C-deficient mice grow well, but branch poorly in organ culture. Am. J. Respir. Cell Mol. Biol. 30, 360–366.
Saga, Y., Yagi, T., Ikawa, Y., Sakakura, T., Aizawa, S., 1992. Mice develop normally without tenascin. Genes Dev. 6, 1821–1831.
Shima, H., Tsuji, M., Elfman, F., Cunha, G.R., 1995. Development of male urogenital epithelia elicited by soluble mesenchymal factors. J. Androl. 16, 233–241.
Shiraishi, T., Kato, H., Komada, S., Imai, H., Hirokawa, Y., Kusano, I., Yatani, R., Sakakura, T., 1994. Tenascin expression and postnatal development of the human prostate. Int. J. Dev. Biol. 38, 391–395.
Simian, M., Hirai, Y., Navre, M., Werb, Z., Lochter, A., Bissell, M.J., 2001. The interplay of matrix metalloproteinases, morphogens and growth factors is necessary for branching of mammary epithelial cells. Development 128, 3117–3131.
Stukenberg, P.T., 2004. Triggering p53 after cytokinesis failure. J. Cell Biol. 165, 607–608.
Sugimura, Y., Cunha, G.R., Donjacour, A.A., 1986. Morphogenesis of ductal networks in the mouse prostate. Biol. Reprod. 34, 961–971.
Takeda, H., Oike, Y., Sakakura, T., 1988. Immunofluorescent localization of tenascin during development of the mouse urogenital sinus: possible involvement in genital duct morphogenesis. Differentiation 39, 131–138.
Tamaoki, M., Imanaka-Yoshida, K., Yokoyama, K., Nishioka, T., Inada, H., Hiroe, M., Sakakura, T., Yoshida, T., 2005. Tenascin-C regulates recruitment of myofibroblasts during tissue repair after myocardial injury. Am. J. Pathol. 167, 71–80.
Thompson, H.G., Mih, J.D., Krasieva, T.B., Tromberg, B.J., George, S.C., 2006. Epithelial-derived TGF-beta2 modulates basal and wound-healing subepithelial matrix homeostasis. Am. J. Physiol. Lung Cell. Mol. Physiol. 291, L1277–L1285.
Thompson, T.C., Cunha, G.R., Shannon, J.M., Chung, L.W., 1986. Androgen-induced biochemical responses in epithelium lacking androgen receptors: characterization of androgen receptors in the mesenchymal derivative of urogenital sinus. J. Steroid. Biochem. 25, 627–634.
Tomas, D., Ulamec, M., Hudolin, T., Bulimbasic, S., Belicza, M., Kruslin, B., 2006. Myofibroblastic stromal reaction and expression of tenascin-C and laminin in prostate adenocarcinoma. Prostate Cancer Prostatic Dis. 9, 414–419.
Tremblay, L., Hauck, W., Nguyen, L.T., Allard, P., Landry, F., Chapdelaine, A., Chevalier, S., 1996. Regulation and activation of focal adhesion kinase and paxillin during the adhesion, proliferation, and differentiation of prostatic epithelial cells in vitro and *in vivo*. Mol. Endocrinol. 10, 1010–1020.
Tuxhorn, J.A., Ayala, G.E., Smith, M.J., Smith, V.C., Dang, T.D., Rowley, D.R., 2002. Reactive stroma in human prostate cancer: induction of myofibroblast phenotype and extracellular matrix remodeling. Clin. Cancer Res. 8, 2912–2923.
Vollmer, G., Michna, H., Ebert, K., Knuppen, R., 1994a. Androgen ablation induces tenascin expression in the rat prostate. Prostate 25, 81–90.
Vollmer, G., Michna, H., Schneider, M.R., Knuppen, R., 1994b. Stromal expression of tenascin is inversely correlated to epithelial differentiation of hormone dependent tissues. J. Steroid Biochem. Mol. Biol. 48, 487–494.
Weaver, V.M., Lelievre, S., Lakins, J.N., Chrenek, M.A., Jones, J.C., Giancotti, F., Werb, Z., Bissell, M.J., 2002. beta4 integrin-dependent formation of polarized three-dimensional architecture confers resistance to apoptosis in normal and malignant mammary epithelium. Cancer Cell. 2, 205–216.
Wu, C.T., Altuwaijri, S., Ricke, W.A., Huang, S.P., Yeh, S., Zhang, C., Niu, Y., Tsai, M.Y., Chang, C., 2007. Increased prostate cell proliferation and loss of cell differentiation in mice lacking prostate epithelial androgen receptor. Proc. Natl. Acad. Sci. U. S. A. 104, 12679–12684.
Xue, Y., Li, J., Latijnhouwers, M.A., Smedts, F., Umbas, R., Aalders, T.W., Debruyne, F.M., De La Rosette, J.J., Schalken, J.A., 1998. Expression of periglandular tenascin-C and basement membrane laminin in normal prostate, benign prostatic hyperplasia and prostate carcinoma. Br. J. Urol. 81, 844–851.